

PAPER • OPEN ACCESS

Daily performance of a solar hybrid regenerative gas turbine in Colombia

To cite this article: F Moreno-Gamboa *et al* 2021 *J. Phys.: Conf. Ser.* **2073** 012012

View the [article online](#) for updates and enhancements.

You may also like

- [Experimental study of 2-layer regenerators using Mn-Fe-Si-P materials](#)
T V Christiaanse, P V Trevizoli, Sumohan Misra et al.
- [Investigating student understanding of a heat engine: a case study of a Stirling engine](#)
Lilin Zhu and Gang Xiang
- [Experimental investigation of MnFeP_{1-x}As_x multilayer active magnetic regenerators](#)
P Govindappa, P V Trevizoli, O Campbell et al.



The Electrochemical Society
Advancing solid state & electrochemical science & technology

243rd ECS Meeting with SOFC-XVIII

More than 50 symposia are available!

Present your research and accelerate science

Boston, MA • May 28 – June 2, 2023

[Learn more and submit!](#)

Daily performance of a solar hybrid regenerative gas turbine in Colombia

F Moreno-Gamboa¹, E Vera-Duarte¹, and G Guerrero-Gómez²

¹ Grupo de Investigación en Fluidos y Térmicas, Universidad Francisco de Paula Santander, San José de Cúcuta, Colombia

² Grupo de Investigación en Tecnología y Desarrollo en Ingeniería, Universidad Francisco de Paula Santander, Seccional Ocaña, Colombia

E-mail: faustinomoreno@ufps.edu.co

Abstract. This work presents the evolution of the operation of a regenerative hybrid solar gas turbine in an average day of the year. The system is evaluated by means of a thermodynamic model that includes a solar concentrated heliostat field solar concentrator with central receiver, a combustion chamber, and the thermal engine. The model is applied in Barranquilla, Colombia using local temperature and the solar radiation estimated with a theoretical model. Power output, the global efficiency and thermal engine efficiency are estimated. Additionally, to estimate the temperatures in different states of the cycle with and without regenerator. Finally, the impact of the regenerator is evaluated, which can increase the temperature of the solar receiver by up to 13.6%, and the inlet temperature to the combustion chamber increases by 17.3% at noon, when solar radiation is maximum.

1. Introduction

The growth in energy demand associated with population growth and industrial development reinforces the need to develop new means of energy production that allow the reduction of polluting emissions. concentrated solar power (CSP) are systems that concentrate solar energy to supply heat to a working fluid within a power cycle and can help meet current energy needs [1]. The CSP systems coupled to gas turbines stand out for their flexibility in terms of possible configurations, reliability in operation and scalability in size and generation capacity [2].

In hours without solar resource, several alternatives have been developed as energy sources, among them, thermal storages whose main restriction is the low operating temperature, which makes them very useful in Rankine cycles [3]. To meet the high temperature requirements of Brayton cycles, it is possible to use hybridization [4], which involves incorporating a combustion chamber, which should be controlled to achieve an approximately constant turbine inlet temperature independent of solar resource variations and guaranteeing continuous operation when radiation is not present [5]. An interesting solar concentration option for this type of system is the heliostat field and tower with central receiver, which is very well adapted to the inclusion of combustion chamber [6]. At the experimental level, a megawatt-scale plant called Solugas has been developed with a 4.6 MW Mercury 50 gas turbine [7] and will serve as a reference for this work.

This paper presents a model has irreversibilities in its components and a basic analysis of the solar concentration. Additionally, with few parameters it allows evaluating temperatures, efficiency, and power. Finally, an analysis of the plant under atmospheric conditions of Barranquilla, Colombia, is



presented, showing the evolution of the main operating parameters of the plant throughout a day, such as power, efficiencies, and temperatures.

2. Solar hybrid thermal power plant and models

This section presents the schematic of hybrid solar turbine and then describes the solar resource estimation model and the thermodynamic model of the plant operation.

2.1. Overall plant model

The configuration of a closed-cycle hybrid CSP plant operating with air Figure 1(a) and temperature vs. entropy diagram Figure 1(b) is observed. The plant layout consists of a compressor (process 1-2), a regenerator (process 2-x). Next, a solar receiver (process x-y) receives concentrated irradiation from heliostat field and delivers heat to the air through a heat exchanger. This is followed by a combustion chamber (process y-5) that burns natural gas. The working fluid reaches turbine (process 3-4) and ambient heat exchanger (process 1-z).

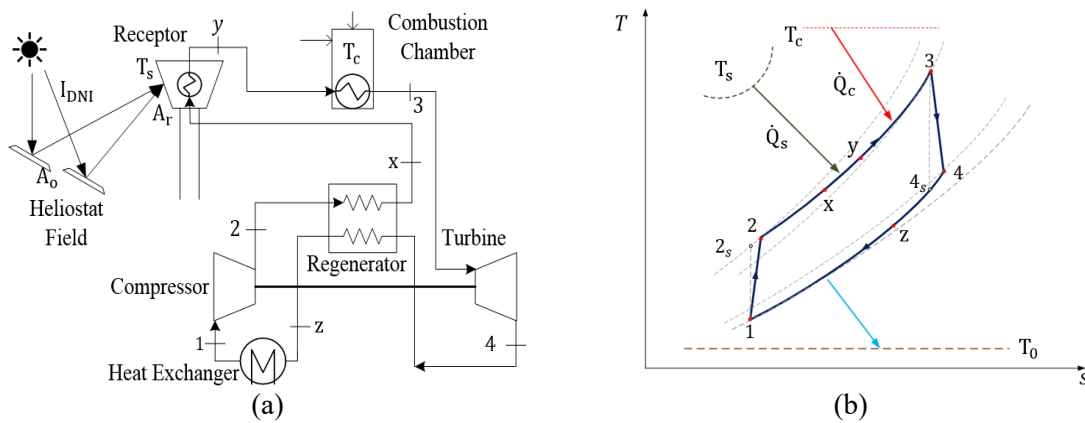


Figure 1. (a) scheme of the solar hybrid gas-turbine plant; (b) temperature-entropy diagram.

2.2. Solar estimation model

In Colombia, there is no access to direct solar radiation data in many parts of the country, and given the need to estimate the solar resource, it is feasible to use models such as the one developed by Gueymard (DI model) [8]. In DI model, the hour to day relationships for diffuse r_d and global r_t radiation is introduced. Additionally, \bar{D}_h and \bar{H}_h represent long-term monthly daily averages for global and diffuse radiation. Direct solar radiation I_B , can be estimates with Equation (1) [8].

$$I_B = r_t \bar{H}_H - r_d \bar{D}_H, \quad (1)$$

2.3. Power plant thermodynamic model

Based on the work carried out by Moreno et al [9] and according to system diagram, the thermodynamic model is described below. The solar concentrating system efficiency can be defined by the Equation (2) [9]. Where A_o and A_r represent the area of heliostat field and central receiver respectively, T_s is the temperature of central tower receiver, U_l is conduction and conversion heat transfer coefficient, α is the central receiver emissivity, σ is the Stefan-Boltzmann constant and η_0 is the optical efficiency of the heliostat field.

$$\eta_{cs} = \left(I_B A_o - I_B A_o (1 - \eta_0) - A_r (U_l (T_s - T_0) + \alpha \sigma (T_s^4 - T_0^4)) \right) / (I_B A_o). \quad (2)$$

In the central tower receiver, heat is delivered to the working fluid, by means of a heat exchanger with effectiveness ϵ_s ; both defined in Equation (3) and Equation (4) [9].

$$\varepsilon_s = (T_y - T_x)/(T_s - T_x), \quad (3)$$

$$\dot{Q}_s = \dot{m} (h_y - h_x). \quad (4)$$

The ultimate heat supply is given in the combustion chamber \dot{Q}_c and heat exchanger of the combustion chamber ε_c can be evaluated by Equation (5) and Equation (6) [9], where η_{cc} is the combustor efficiency, Q_{lhv} is the lower heating value of the fuel and \dot{m}_f is the mass flow rate of the fuel

$$\dot{Q}_c = \eta_{cc} \varepsilon_c Q_{lhv} \dot{m}_f = \dot{m} (h_3 - h_y), \quad (5)$$

$$\varepsilon_c = (T_3 - T_y)/(T_c - T_y). \quad (6)$$

Also, is defined the total heat supplied (\dot{Q}_h) to the working fluid (see Equation (7)) and solar factor (see Equation (8)).

$$\dot{Q}_h = \dot{Q}_c + \dot{Q}_s = \dot{m} (h_3 - h_x), \quad (7)$$

$$f = \dot{Q}_s/\dot{Q}_H = \dot{Q}_s/(\dot{Q}_c + \dot{Q}_s). \quad (8)$$

In addition, the cycle releases heat to the environment \dot{Q}_a , with an effectiveness ε_a , which is expressed in Equation (9) and Equation (10) [9].

$$\dot{Q}_a = \dot{m} (h_z - h_1), \quad (9)$$

$$\varepsilon_a = (T_1 - T_z)/(T_0 - T_z). \quad (10)$$

The efficiency of the thermal machine or power cycle η_{mt} , and the power output of the solar thermal plant, P_n are evaluated for Equation (11) and Equation (12) [9].

$$P_n = \dot{m} ((h_3 - h_4) - (h_2 - h_1)), \quad (11)$$

$$\eta_{mt} = P_n / \dot{Q}_H. \quad (12)$$

The overall efficiency of plant is estimated in Equation (13) [9].

$$\eta = P_n / (\dot{m}_f Q_{lhv} + I_B A_o), \quad (13)$$

Finally, the fuel conversion factor (see Equation (14)) [9] of plant is defined as the power generated over the heat of the fuel consumed [2].

$$r_f = P_n / (\dot{m}_f Q_{lhv}). \quad (14)$$

3. Result and discussion

This section presents the validation of the DI model and thermodynamic model. Additionally, the results of the evolution of the operation of the hybrid solar turbine are presented.

3.1. Validation models

This section presents the validation of the models. Due to the lack of publicly available I_B data in Colombia, the DI model is initially evaluated with data reported for Seville. The data obtained with the DI model and those obtained in Meteosevilla website are compared by means of mean absolute bias error (MABE) with a value of 0.2010085 and root mean square error (RMSE) with a value of 0.226616, which are considered acceptable according to the literature [10]. Regarding the thermodynamic model, the validation results are presented in Table 1 with maximum errors of 1% which indicates a strong correlation of the model.

Table 1. Thermodynamic model assessment.

	P_n	η_{MT}	T_3 (K)	T_4 (K)
Model	4635.4	0.385	1422	914
Reference	4600 [11]	0.39 [11]	1423 [2]	921 [2]
Error %	0.7	1	0.07	0.7

3.2. Simulation and results analysis

The variation of the power output of the plant over the average day of the year with respect to the hourly average ambient temperature it shows in Figure 2 [12]. Where the power is strongly influenced by the ambient temperature because a reduction in T_0 implies an increase in the net power given the increase in the ratio between the maximum and minimum temperature of the cycle. The relative amplitude of the power output is 3% and the solar radiation has no effect on the power output. Plant efficiencies have been evaluated over the average day of the year and these curves are shown in Figure 3. Thermal engine efficiency η_{mt} remains almost constant as it depends on \dot{Q}_h and P_n . The influence of combustion chamber efficiency and the solar concentration system is not observed and η_{mt} it reaches an average value of 33.3%.

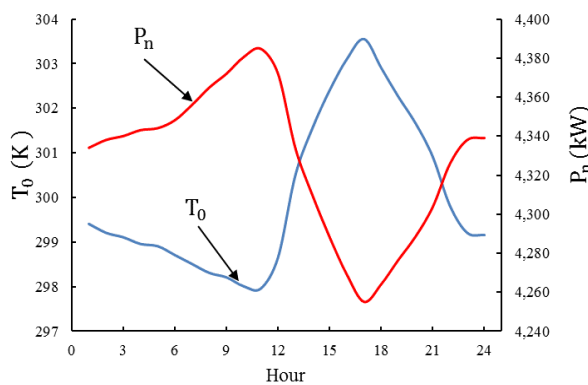


Figure 2. Evolution of ambient temperature and plant power during the day.

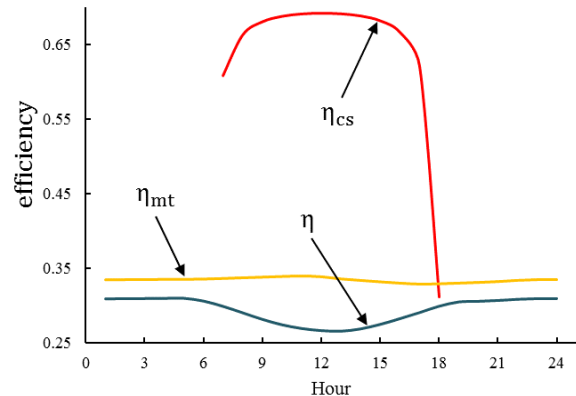


Figure 3. Evolution of plant efficiencies over the day.

The overall efficiency of the plant, in addition to being influenced by the combustion chamber system, is significantly impacted by the solar concentrator system and its efficiency, which is why it is observed that in the central hours of the day η decreases as a result of energy losses in the solar concentrator. In the case of Barranquilla, the hours of influence of the solar concentrator do not vary much on the year since the sunrise and sunset times barely vary by 33 minutes throughout the year and the influence of the seasons is not present. The same happens with the solar noon which varies around

12 m throughout the year and at this time for the simulated average day. The average value of η at night is 30.7% and at noon it is 26.2%, a reduction of 14.6%.

Heliostat field efficiency is a function of cosine effect, blocking factor, attenuation, and shading, along with mirror reflectivity. However, the basic solar concentrator model used takes a global average value of the optical efficiency ($\eta_0 = 0.73$ [13]) and nonlinear losses in the central tower receiver, without being a dynamic model. Figure 3 shows the evolution of η_{cs} shown only when the system can provide effective energy to the cycle, significant variations are observed in the morning and in the afternoon but around noon. The curve forms a plateau due to the increase of the losses in the solar receiver that are a function of T_s and in which η_0 does not vary, despite the increase of I_B . At noon η_{cs} has a value of 69.1%.

Figure 4(a) shows the evolution of the operating temperatures of the plant throughout the day without regenerator, which logically does not include the regenerator outlet temperatures (T_x and T_z). The compressor outlet temperature, T_2 , varies due to the influence of ambient temperature as does the compressor inlet temperature T_1 , both varying around 700 K and 305 K respectively. The tower receiver takes the air from T_2 to T_y reaching a maximum value of 856 K and presenting a profile similar to that of T_s and I_B . Additionally, the turbine inlet temperature T_3 is kept almost constant due to the operation of the combustion chamber at values around 1420 K, which ensures that P_n is also almost constant.

Figure 4(b) shows the evolution of the operating temperatures of the plant operating with regenerator ($\epsilon_r = 0.77$), as well as the regenerator outlet temperatures T_x and T_z with average values of 852 K and 706 K, respectively. The above shows the reduction in fuel consumption since the combustion chamber must provide heat from T_x and not from T_2 as it did without the regenerator. Finally, the solar receiver temperature reaches a maximum value of 1038 K and T_y of 1000 K.

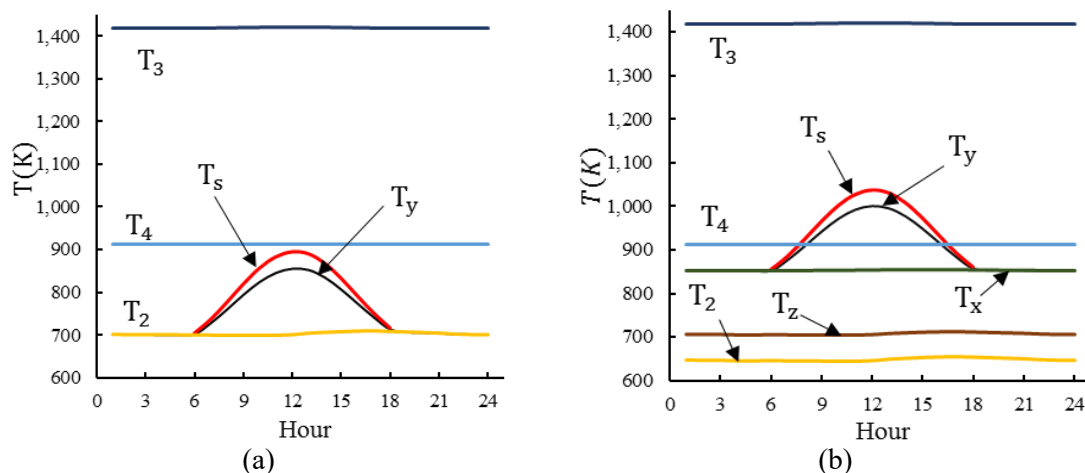


Figure 4. Evolution of the plant temperatures; (a) without regenerator; (b) with regenerator.

According to the temperature variation in the operation of the plant, a direct effect on the reduction of fuel consumption can be seen when part of the energy required by the plant is supplied by the solar concentrator, as shown in Figure 5(a), which shows the evolution of the fuel consumption (\dot{m}_f) of the plant during the day of operation with the regenerator ($\epsilon_r = 0.77$). At night, fuel consumption varies as a function of ambient temperature, but when the solar resource is available, \dot{m}_f is reduced as a function of the increased concentrator input. Figure 5(a) presents the consumption without solar concentrator (dashed red line) and with the solar concentrator blue line, the area between the two lines is the daytime fuel savings, which is estimated at 6.3%.

Figure 5(b) shows the fuel conversion factor r_f , which remains approximately constant during nighttime hours given the minimum variation in power and fuel consumption, but with the solar contribution reaching a maximum value of 0.42. Additionally, the solar factor, which goes from zero at night to a maximum value of 0.2546 at midday, indicates that the concentration system studied contributes a maximum of 25% of the heat received by the power cycle.

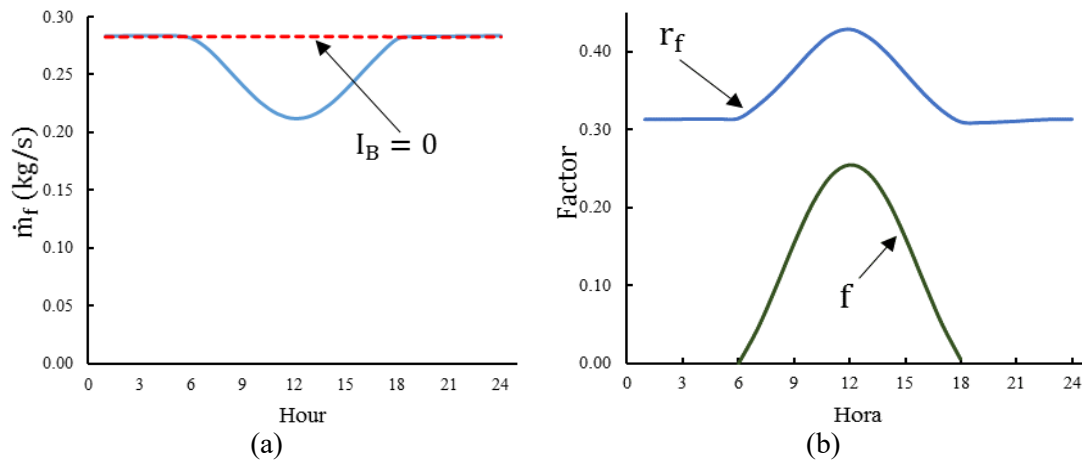


Figure 5. Evolution of fuel consumption; (a) solar factor; (b) fuel conversion rate.

4. Conclusions

A thermodynamic model of a thermal plant coupled to a solar hybrid system is presented, which has a model for estimating direct solar radiation, which allows estimating the operating conditions of the plant at any place and time of the year. Additionally, the model supports the ambient temperature of the site and the temperature of the combustion chamber. The model also allows evaluating the operation of the plant in different configurations, such as the elimination of the solar concentrator chamber and the regenerator.

The Solugas experimental plant was used as a reference to evaluate the model and its possible operation in the city of Barranquilla, Colombia. It is observed that technically the plant can operate in this city, however, an optimization of the heliostat field and the configuration of the solar concentration system is required, considering the possible variations in the distribution of the heliostats and the total size of the field, in order to evaluate in detail its efficiency.

The concentrating solar power system can achieve a daily fuel consumption savings of 7.7% being in the range estimated (between 4% and 11.7%) for the same configuration at Solugas, Spain. However, a detailed analysis of the solar concentration system, especially the optical efficiency and the adequate distribution of the heliostat field for the city of Barranquilla, where the application of this type of technology is feasible, is deemed convenient.

Acknowledgments

The authors thank the Universidad Francisco de Paula Santander, Colombia, for facilitating the Dymola license.

References

- [1] Goswami Y 2015 *Principles of Solar Engineering* (Boca Raton: CRC Press)
- [2] Santos M J, Merchán R P, Medina A, Calvo Hernandez A 2016 Seasonal thermodynamic prediction of the performance of a hybrid solar gas-turbine power plant *Energy Conversion and Management* **115** 89
- [3] Jokar M A, Ahmadi M H, Sharifpur M, Meyer J P, Pourfayaz F, Ming T 2017 Thermodynamic evaluation and multi-objective optimization of molten carbonate fuel cell-supercritical CO₂ Brayton cycle hybrid system *Energy Conversion and Management* **153** 538
- [4] Bernardos E, López I, Rodríguez J, Abánades A 2013 Assessing the potential of hybrid fossil-solar thermal plants for energy policy making: Brayton cycles *Energy Policy* **62** 99
- [5] Merchán R P, Santos M J, Medina A, Calvo Hernández A 2018 Thermodynamic model of a hybrid Brayton thermosolar plant *Renewable Energy* **128** 473
- [6] Nathan G J, Jafarian M, Dally B, Saw W L, Ashman P J, Hu E, Steinfeld A 2018 Solar thermal hybrids for combustion power plant: A growing opportunity *Progress in Energy and Combustion Science* **64** 4
- [7] Korzynietz R, Brioso J, Del Rio A, Quero M, Gallas M, Uhlig R, Ebert M, Buck R, Teraji D 2016 Solugas - Comprehensive analysis of the solar hybrid Brayton plant *Solar Energy* **135** 578

- [8] Gueymard C A 2000 Prediction and performance assessment of mean hourly global radiation *Solar Energy* **68(3)** 285
- [9] Moreno F, Escudero A, Nieto C 2020 Performance evaluation of external fired hybrid solar gas-turbine power plant in Colombia using energy and exergy methods *Thermal Science and Engineering Progress* **20** 100679
- [10] Mejdoul R, Taqi M 2012 The mean hourly global radiation prediction models investigation in two different climate regions in Morocco *International Journal of Renewable Energy Research* **2(4)** 608
- [11] Olivenza-León D, Medina A, Calvo Hernández A 2015 Thermodynamic modeling of a hybrid solar gas-turbine power plant *Energy Conversion and Management* **93** 435
- [12] Ramírez-Cerpa E, Acosta-Coll M, Vélez-Zapata J 2017 Análisis de condiciones climatológicas de precipitaciones de corto plazo en zonas urbanas: caso de estudio Barranquilla, Colombia *Idesia* **35(2)** 87
- [13] Romero M, Steinfeld A 2012 Concentrating solar thermal power and thermochemical fuels *Energy & Environmental Sciences* **5(11)** 9234